Quantification of ESD Pulses Caused by Collision of Objects

Gabriel Fellner
Institute of Electronics
Graz University of Technology
Graz, Austria
gabriel.fellner@tugraz.at

Amin Pak
Institute of Electronics
Graz University of Technology
& SAL Graz EMC lab
Graz, Austria
amin.pak@tugraz.at

Seyed Mostafa Mousavi
Institute of Electronics
Graz University of Technology
Graz, Austria
seyedmostafa.mousavi@tugraz.at

Christoph Koger
Institute of Electronics
Graz University of Technology
Graz, Austria
christoph.koger@student.tugraz.at

Ali Khorrami
Apple Inc.
Cupertino, USA
mkhorrami@apple.com

David Pommerenke
Institute of Electronics
Graz University of Technology
& SAL Graz EMC lab
Graz, Austria
david.pommerenke@tugraz.at

***Abstract*—Well-insulated portable devices are exposed to field coupled impulsive ESDs if they are carried e.g., in a backpack. These pulses are created by tribo-charging of metallic objects as a result of movement and subsequent discharges. Due to the size of the metallic objects and low charge voltages, the frequency spectrum exceeds 5 GHz. The pulses can damage or upset devices. The paper quantifies the charge voltages and transient field strength by reproducing typical scenario and capturing transient fields with a bandwidth of more than 10 GHz. The charge voltages are estimated by comparing measurements to numerical modeling of the discharges.**

Keywords—Electrostatic discharge (ESD), tribo-charging

I. Introduction

Electrostatic discharges can lead to soft- and hard errors in systems. Most systems are tested according to the IEC 61000-4-2 standard. The standard uses 850 ps rise time pulses as reference event [1]. Actual ESD can have much lower rise times, especially at low voltages and fast approach speeds [2]. The associated RF spectrum can reach up to 10 GHz and is beyond the spectrum the product is exposed to during standardized testing. Especially with the proliferation of low current, high speed sensors and antennas in the 1-10 GHz range for mobile devices, there is an increased risk of damage to these devices in normal handling, despite the devices having passed standardized ESD testing. If a product is carried in a backpack and other metallic devices are present then the movement in the backpack can tribo-charge the objects leading to ESDs in close proximity of the device. Depending on the voltages, object size and approach speeds ESDs having endangering energy content in the multi-GHz range can occur. This phenomenon was reported by Doug Smith [3,4] without quantifying the field strengths or charge voltages. Motivated by using the transient fields of charged device model (CDM) ESD Maloney created analytical models that related the discharge to their associated fields. Zeitlhoefler, et.al. used this work to detect CDM events in production [5]. This was based on the characterization of different antennas used for broadband impulse detection [6,7,8]. This paper is analyzing discharges from moving every-day objects, estimates the field strengths based on measurements and uses full wave simulation to estimate the voltages on the discharging objects.

II. Experimental and Numerical Setup

A. Antennas and their performance

A wide choice of broadband antennas has been reported in the sensors and simulation notes over decades. They range from Ddot, Bdot probes to a wide range of TEM field based antennas (TEM-Horn, Vivaldi), disk-cone and include log-per antennas. The Sensors and Simulation Notes provide many designs. We selected Vivaldi antennas for their acceptable pulse fidelity, low cost and robustness as reference antennas.

The RF performance of the antennas is numerically investigated and experimentally verified. A simulation geometry, that models the coupling of a plane wave to the antenna is shown in Fig. *1*.

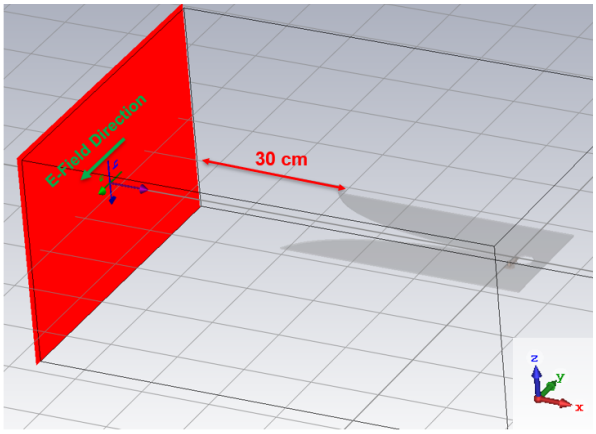

Fig. 1. CST setup for the simulation of the plane wave coupling to the Vivaldi antenna

The results obtained using the setup shown in Fig. 1 can be expressed in multiple ways. The antenna factor, which gives the ratio of the field strength to the voltage at the antenna port is shown in Fig. 2. In the frequency range of interest, about 1 – 10 GHz, its value varies from about 25 dB/m to 37 dB/m.

A time domain analysis investigates the same antenna, but gives deeper in-sight into the coupling of impulsive waveforms into the antenna. If the excitation of the plane wave is switched to a Gaussian pulse of varying width (measured at

978-1-7281-5579-1/20/$31.00 ©2022 IEEE

50 % of the amplitude) the coupling of narrow pulses is visible. Fig. 3 shows the coupled pulses for pulses having a width of 40…1000 ps for a 1 V/m plane wave. On average, 33 mV are coupled for 1 V/m field strength.

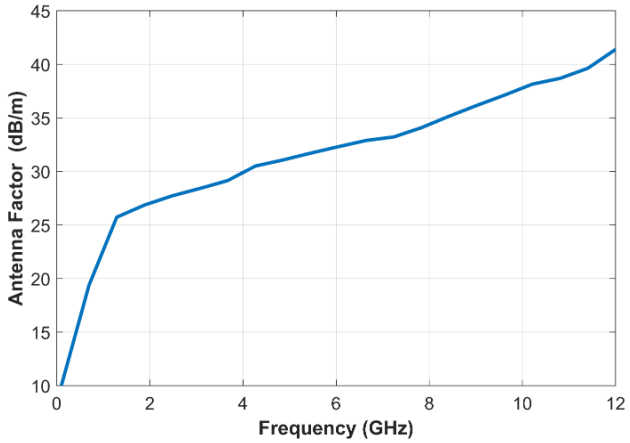

Fig. 2. Antenna factor of the Vivaldi antenna determined using CST full wave simulation. Note: 30 dB/m is 29.5 m^{-1} in linear units

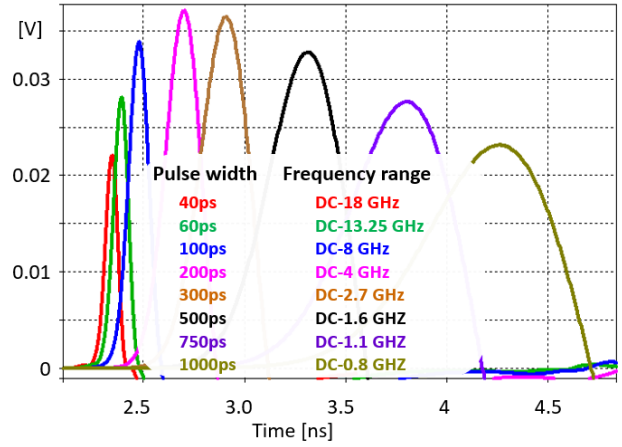

Fig. 3. Output voltage of the Vivaldi antenna for Gaussian pulses of different pulse widths (measured at half amplitude) and 1 V/m field strength

The data in Fig. 3 indicated that an antenna factor of 1/0.033 = 30.3 m^{-1} provides a reasonable broadband conversion of the output voltage of the Vivaldi to the field strength of the signal that reached the antenna. The largest pulses shown in Fig. 7 are about 30 Vp. This indicates 900 V/m at 35 cm distance from the shaking machine. Using 1/r extrapolation leads to an initial rough estimate of 9 kV/m at a distance of 3.5 cm.

B. Creating discharges

Everyday objects are placed into a shaker together with insulating parts and moved in a reproducible fashion, recreating movements that could be observed when carrying objects in a backpack while walking. The radiated fields are captured using a Vivaldi antenna at a distance of 35 cm from the shaker. In most tests the objects include wool, Teflon, screws, and nuts, see Fig. 4. For these objects, it is not possible to predict the geometry during a discharge event. To be able to compare to numerical simulations, additional experiments are performed that only use metallic spheres as discharging objects. Three sizes are used: 20 mm, 40 mm and 55 mm diameter, see Fig. 5.

Fig. 4. Typical objects used in the initial experiments. Experiments have been conducted at about 23°C and 50 % RH. Future experiments will consider lower humidities.

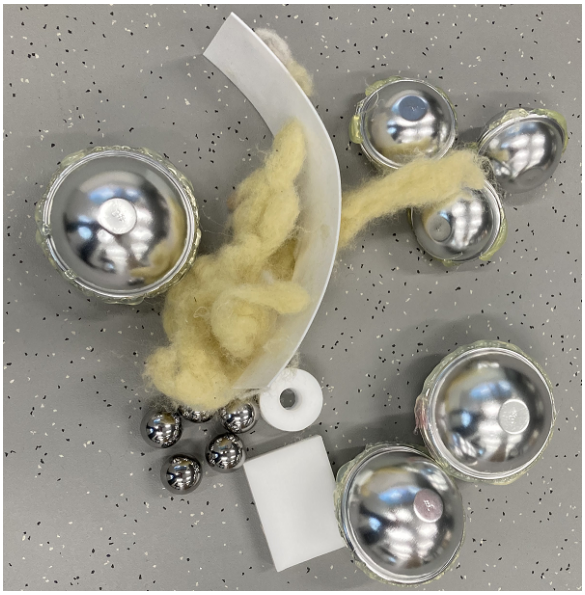

Fig. 5. Spheres of different size, wool, Teflon and other plastic materials used in experiments using spheres to define the geometry of collisions. In each experiment only one sphere size was used.

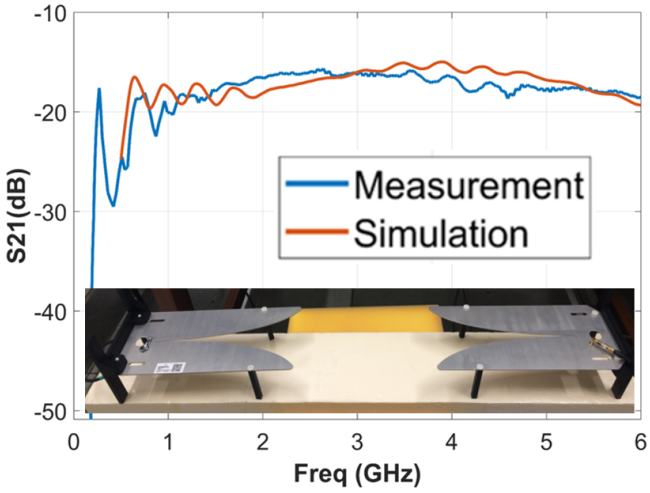

Fig. 6. S21 of two Vivaldi antennas, simulation and measurement

The S21 between two Vivaldi antennas was measured and simulated. The data in Fig. 6 indicate a good match. This gives support to the accuracy of the simulated discharge data.

III. Results

A. Time domain

Results of voltages from the first tests using the material shown in Fig. 4 are presented in Fig. 7. The data was captured using a 33 GHz scope, however, the frequency content larger than 12 GHz is very low. Data sets using the 12 GHz and the 33 GHz scope are similar. The data in Fig. 7 indicates voltages up to 30 V induced into the Vivaldi antenna at 35 cm distance.

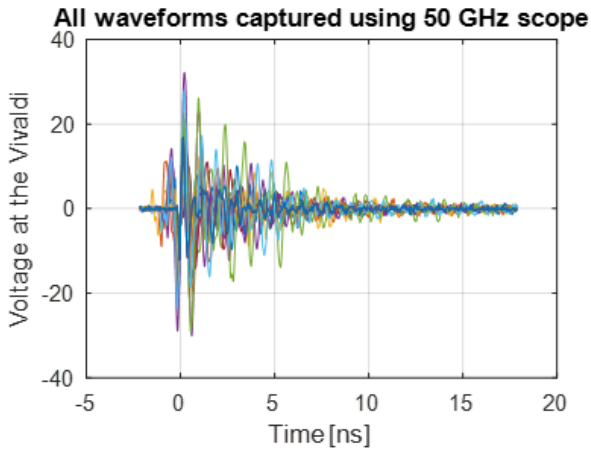

Fig. 7. Voltages induced in the Vivaldi antenna at a distance of 35 cm from the shaking using the objects shown in Fig. 4.

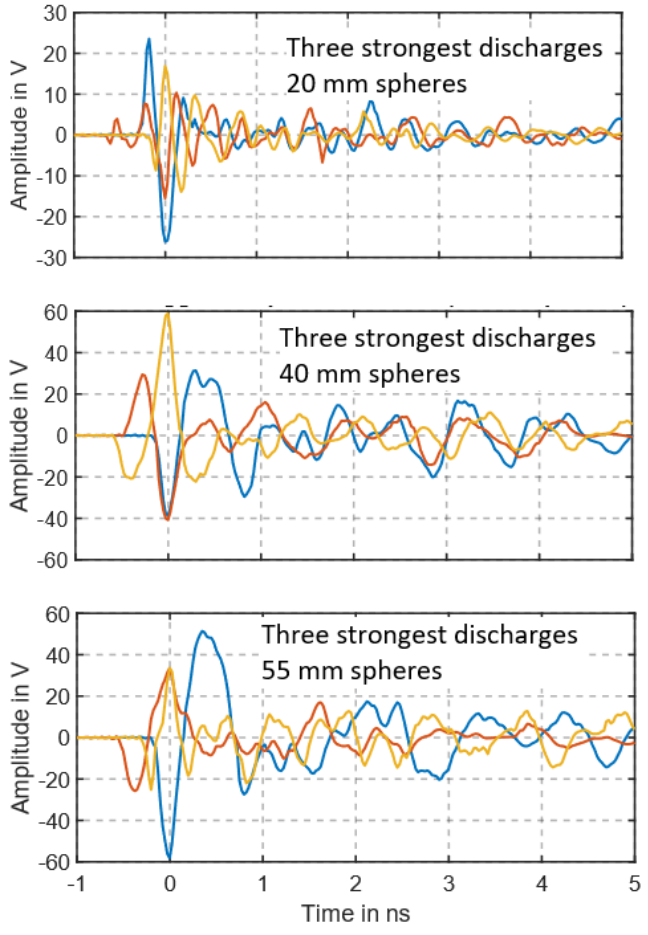

Fig. 8. Example waveforms as captured by the Vivaldi from the data set shown in Fig. 15. Note: Larger discharge waveforms are selected as they pose the most risk to electroinc devices. Data taken at: 23°C about 50% RH

Individual waveforms for discharges using the spheres are shown in Fig. 8, which were captured with the materials shown in Fig. 5. They indicate that the induced voltages form narrow, less than 500 ps wide pulses similar to the data reported in [6,7]. The actual current pulse is a narrow unipolar pulse. Its shape can be compared with the shape of Charged Device Model pulses from discharging integrated circuits [5,6,7]. Due to the derivative relationship between the current and the received field a signal with both a positive and a negative pulse is received. Larger spheres give wider pulses as the discharge current flows for a longer time period.

B. Spectral composition

The spectral content, extracted from the voltage induced in the Vivaldi antenna extends beyond 8 GHz. It is a function of the size of the discharging objects, see Fig. 9.

The data in Fig. 9 shows the "max-hold" spectrum of the power spectrum of 3000 discharges, 1000 each for each ball size. The data indicate spectral components above the noise floor up to 10 GHz for all spheres. It is not surprising that, the smaller spheres provide less low frequency energy. The observed spectral energy drops for all spheres below 800 MHz. This might be native to the discharge even of the larger spheres but certainly, it is influenced by the lower cut-off of the Vivaldi antenna.

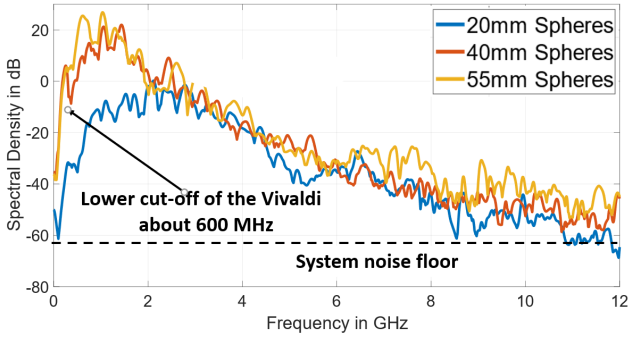

Fig. 9. Max-hold relative spectral density of the impulse data captured by the Vivaldi antenna, including system noise floor. Note the effect of the lower cut-off frequency of the antenna.

IV. Calibration to Estimate the Charge Voltages

In a random shaking experiment the orientation of the impulsive currents relative to the antenna polarization is not controlled. Furthermore, the fields can be reflected by the other parts inside the shaking structure. A more controlled experiment allows a direct comparison to simulation.

To estimate the voltages between the metal parts prior to a discharge we reference the measured data back to a numerical model. The model simulates discharges between two spheres and captures the field induced in the Vivaldi antenna model. The simulation geometry is shown in Fig. 10. The excitation is achieved by defining a voltage discrete port in series with a resistor and placing this serial connection between the two spheres. The resistor models the discharge resistance and is excited by a step function. The CST time domain solver is used.

Different sizes of the spheres have been used in this study. Obviously, larger spheres lead to stronger fields and slower ringing, Fig. 11. The ringing frequency equals the natural resonance of the geometry and the decay is govern by radiation loss and loss in the spark resistance. Spacing

between the spheres is important, if it approaches zero, the capacitance converges to infinity. We set the spacing between the spheres to 0.1 mm. Based on Paschen's law we use a spark distance of 0.1 mm for a voltage of 1000 V.

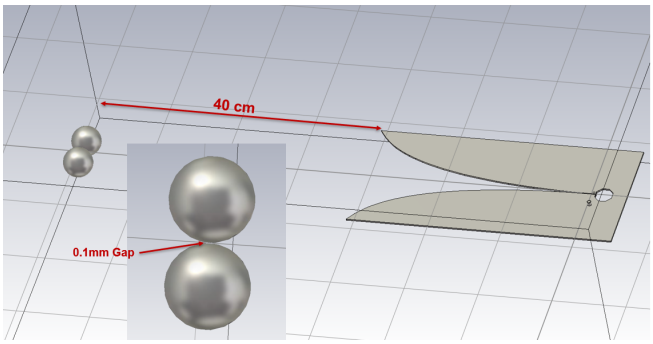

Fig. 10. Simulation model in CST. Two sphere, placed at a distance of 0.1 mm are excited by a step function with picosecond risetime. The radiated field is captured by the Vivaldi antenna

As mentioned, another important effects is the spark resistance. So far, we have not used a time dependent spark resistance equation and we used fixed resistor values instead. The strong effect of the spark resistance is shown in Fig. 12. Increasing it from 10 to 25 Ohm reduces the peak value from 20 V to 12 V and a value of 100 Ohm leads to only 5 V induced voltage. At present, it is difficult to determine the most realistic value. An indication is given from work on CDM simulators, here resistor values from 10 – 25 Ohm give better match to measured data.

The data presented in Fig. 7 and in Fig. 8 shows a maximal voltage induced in the Vivaldi of 30 V for a similar geometry. This allows an estimate that the voltages reach about 1500 V. This justifies our assumption of 0.1 mm spark length. In addition it provides the basis for simulating the currents induced in portable devices at any distance requested.

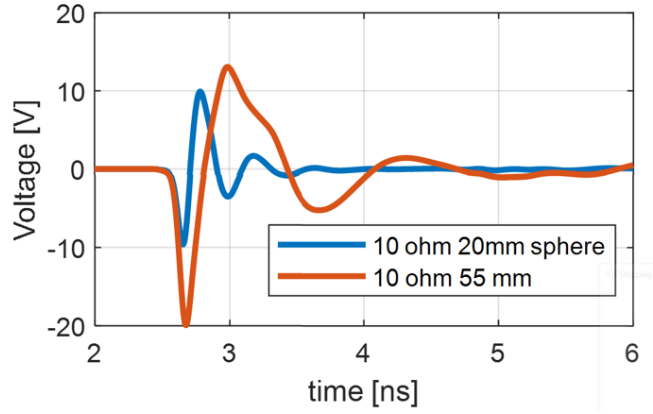

Fig. 11. Voltage induced in the Vivaldi antenna for the discharge between two spheres. Red: Two 20 mm spheres, Blue: Two 55 mm spheres. Are resistance is assumed to be 10 Ohm, scaled to simulate a 500 V discharge

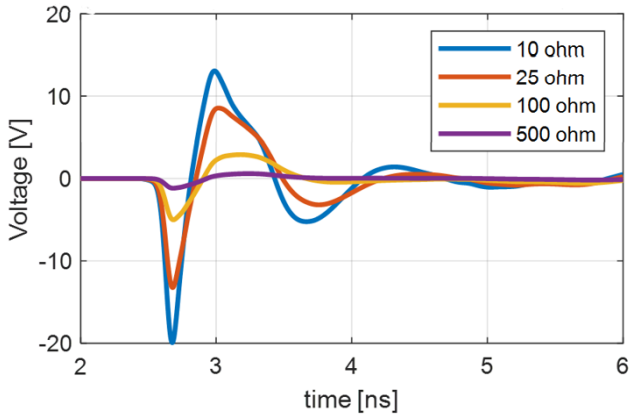

Fig. 12. Voltages induced in the Vivaldi antennas for the discharge between two 55 mm spheres assuming constant arc resistances from 10 to 500 Ohm.The data is scaled to simulate a 500 V discharge.

V. Verification by a Controlled Experiment

To verify the simulation results by experiment, spheres have been charged and dropped while capturing the voltage induced in the Vivaldi antenna. At a voltage of 500 V the discharge induces a voltage of about 10 V into the Vivaldi at 35 cm distance, see Fig. 13. Using the average antenna factor of 30, this indicates a field strength of 300 V/m. Both simulation and measurements agree. Here it is important to ensure that the voltage at the spheres is kept constant. A high resistive wire connects to a power supply. Without this, the voltage would vary due to:

- Change of capacitance, see Fig. 14
- Corona like pre-discharges prior to the main discharge.
- Variations of the spark resistance as shown Fig. 12

Such effects have been extensively observed in monitoring the discharge of spheres that had been pre-charged and then dropped to initiate a discharge without having them connected to a source via high impedance wires.

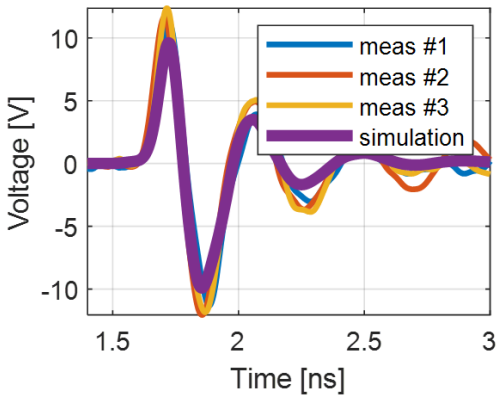

Fig. 13. Simulated and measured field captured by the Vivaldi antenna for a discharge between two 20 mm spheres at 500 V against simulation. To avoid the change of the capacitance and consequently the voltage, the sphere is conneted to a power supply using highly resistive wires. This ensures a voltage of 500 V at the moment of the discharge. Experimentally, it was shown that the drop at 500 V led to rather repeatable waveforms, indicating a short spark length and a low spark resistance. The simulation used 10 Ohm. No attempt was made to use a time dependent spark resistance yet.

If the capacitance change with distance to GND and the consequential change of the voltage is not taken into account

a wrong voltage at the moment of the discharge is assumed. The simulated change of the capacitance with distance is shown in Fig. 14.

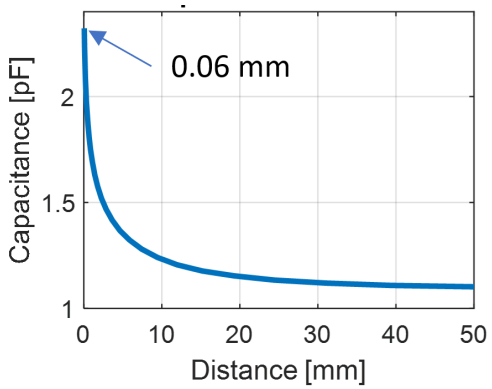

Fig. 14. Capacitance between two spheres as a function of spacing between them. If the sphere is charged to a given voltage and the distance decreases, the voltage will reduce due to the increased capacitance.

For a sphere of 20 mm diameter the capacitance changes from 1.1 pF at 50 mm height to 2.7 pF at 0.06 mm. To place the smallest distance into a general picture it is worth to look at the sparking distances. For 1 kV, using Paschen's law (this means no shortening of the spark length due to statistical time lag and approach speed) a value of 0.1 mm would be observed, for 500 V, 0.06 mm would be expected. Thus, the value range is reasonable, but the exact spark length values are not known. The distribution of the field strength of multiple discharges is shown in Fig. 15. A total of 3000 discharges have been captured, 1000 for each sphere size. The peak value of the induced voltage into the Vivaldi antenna was taken and converted to an estimation of the field strength using the antenna factor. The distribution shows that most discharges are of lower magnitude. This has two reasons:

- Lower voltages are more likely than higher voltages
- The orientation of the discharge current relative to the polarization of the antenna is strongly mismatched
- The radiation direction of the sphere-to-sphere discharges is away from the antenna. The sphere-to-sphere discharge will radiate similar to a dipole, thus, there is no signal in the direction in line with the centers of the spheres

The smaller sphere caused lower field strengths, as seen in the simulation. There is a slight tendency for the 55 mm sphere to causes stronger pulses compared to those of the 40 mm sphere, however the differences in sphere size is small. The strongest field strengths reached 1700 V/m at 35 cm distance. Extrapolated using 1/r this would expose a mobile system in a distance of 3.5 cm to 17 kV/m for a nanosecond period of time.

The cumulative density functions shows that 10 % of the pulses had values larger than 160 V/m for the 20 mm sphere. For the larger spheres we observed that 10 % of the pulses reached peak values of larger than 360 V/m (40 mm sphere) and 400 V/m (55 mm sphere). The data was taken at 23ºC and about 50 % RH. The effect of humidity on the density functions will be part of a follow-up publication.

Let us select a discharge that caused a 400 V/m pulse for a discharge of two 20 mm spheres. Most discharges have values below it. Using the antenna factor of about 30 a peak voltage of 13 V is calculated. If we compare this to the data shown in Fig. 13, we see that a discharge at 500 V caused a pulse of 10 V. From this we can estimate that the pulse that caused a 400 V/m field strength was caused by a discharge of about 600 V. However, the influences of the spark resistance must be taken into account. It was observed that a discharge of a sphere charged to 1000 V provided a pulse that is larger, but not proportionally larger. We associated this to the increased spark distance and spark resistance. For that reason we consider the calculated discharge voltage only as a first order estimate. From the coupling and destruction perspectives, the local field strengths are of greater importance than the actual discharge voltage.

I. Conclusions

In order to quantify the ESD events caused by the discharge of small objects during everyday handling, a test system has been designed to recreate such discharges in a readily reproducible manner. Reproducibility is achieved either statistically by recording a multitude of random discharges using a defined set of objects and dielectrics, or by using individual balls charged to a fixed voltage by a power supply. The transient fields of these discharges are measured using Vivaldi antennas. To obtain the charging voltages, the system is reproduced in a full-wave simulation model. The model provides the antenna factor of the Vivaldi, which allows estimating the field strength at the antenna location. In addition, defined discharge scenarios are created in a full-wave simulation that creates pulses from known voltage levels. These are used as a reference event to relate the voltage and geometry of the discharge to the output voltage of the antenna. Having established this relationship, the measured antenna output voltage can be used to estimate the charge voltages and their distribution in real experiments. This is a first step in characterizing the exposure of a mobile device if it is placed in such an environment.

Acknowledgment

We wish to acknowledge the contributions and inputs made by Mike Reilly and Rui Mi for this work. We also wish to acknowledge the support by the Graz EMC laboratory to this research.

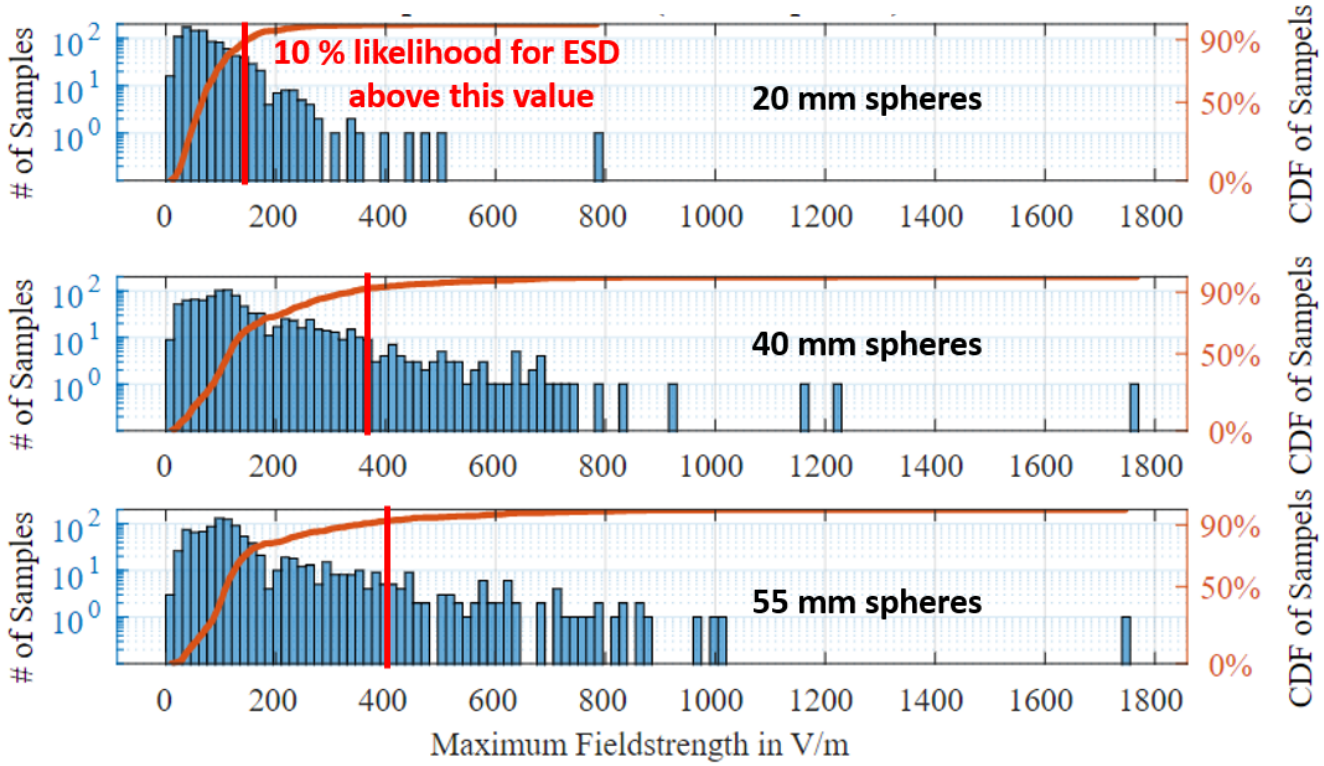

Fig. 15. Histogram of 3000 discharges, 1000 for each sphere size, showing the peak field strength detected by the Vivaldi antenna at a distance of 35 cm defined as the distance from the tip of the Vivaldi to the edge of the material shaker. The cumulative density function (right scale) shows the observed probability of discharges below a field strength value.

REFERENCES

[1] Chundru R, Pommerenke D, Wang K, Van Doren T, Centola FP, Huang JS. Characterization of human metal ESD reference discharge event and correlation of generator parameters to failure levels-part I: Reference event. IEEE Transactions on Electromagnetic Compatibility. 2004 Nov 30;46(4):498-504.

[2] Kawamata K, Minegishi S, Fujiwara O. Radiation characteristics of transient electromagnetic field due to low voltage ESD in spherical electrode. In2014 International Symposium on Electromagnetic Compatibility 2014 Sep 1 (pp. 506-510). IEEE.

[3] Smith DC. Unusual forms of ESD and their effects. InElectrical Overstress/Electrostatic Discharge Symposium Proceedings. 1999 (IEEE Cat. No. 99TH8396) 1999 Sep 28 (pp. 329-333). IEEE.

[4] Yap BC, Patton CR. Investigation of ESD transient EMI causing spurious clock track read transitions during servo-write. InElectrical Overstress/Electrostatic Discharge Symposium Proceedings 2000 (IEEE Cat. No. 00TH8476) 2000 Sep 26 (pp. 233-238). IEEE.

[5] Zeitlhoefler L, zur Nieden F, Gaertner R. ESD risk assessment with Discharge Electrode and Antenna Measurement. In2021 43rd Annual EOS/ESD Symposium (EOS/ESD) 2021 (Vol. 43, pp. 1-10). IEEE.

[6] Zeitlhoefler L, zur Nieden F, Gaertner R. Analysis and Simulation of Antenna Response for Discharge Sensing in Production Environments. In2021 43rd Annual EOS/ESD Symposium (EOS/ESD) 2021 (Vol. 43, pp. 1-10). IEEE.

[7] Maloney TJ. Primary and induced currents from cable discharges. In2010 IEEE International Symposium on Electromagnetic Compatibility 2010 Jul 25 (pp. 686-691). IEEE.

[8] T. J. Maloney, "The Case for Measurement and Analysis of ESD Fields in Semiconductor Manufacturing," *2018 IEEE Symposium on Electromagnetic Compatibility, Signal Integrity and Power Integrity (EMC, SI & PI)*, 2018, pp. 396-401